



Accurate virus quantitation using a Scanning Transmission Electron Microscopy (STEM) detector in a scanning electron microscope



Candace D. Blancett^a, David P. Fetterer^b, Keith A. Koistinen^{a,2}, Elaine M. Morazzani^{c,1}, Mitchell K. Monninger^a, Ashley E. Piper^c, Kathleen A. Kuehl^a, Brian J. Kearney^d, Sarah L. Norris^b, Cynthia A. Rossi^d, Pamela J. Glass^c, Mei G. Sun^{a,*}

^a Pathology Division, United States Army Medical Research Institute of Infectious Diseases (USAMRIID), 1425 Porter Street, Fort Detrick, MD, 21702, United States

^b Biostatistics Division, United States Army Medical Research Institute of Infectious Diseases (USAMRIID), 1425 Porter Street, Fort Detrick, MD, 21702, United States

^c Virology Division, United States Army Medical Research Institute of Infectious Diseases (USAMRIID), 1425 Porter Street, Fort Detrick, MD, 21702, United States

^d Diagnostics Systems Division, United States Army Medical Research Institute of Infectious Diseases (USAMRIID), 1425 Porter Street, Fort Detrick, MD, 21702, United States

ARTICLE INFO

Keywords:

Scanning Transmission Electron Microscopy
Detector
Virus quantitation

ABSTRACT

A method for accurate quantitation of virus particles has long been sought, but a perfect method still eludes the scientific community. Electron Microscopy (EM) quantitation is a valuable technique because it provides direct morphology information and counts of all viral particles, whether or not they are infectious. In the past, EM negative stain quantitation methods have been cited as inaccurate, non-reproducible, and with detection limits that were too high to be useful. To improve accuracy and reproducibility, we have developed a method termed Scanning Transmission Electron Microscopy – Virus Quantitation (STEM-VQ), which simplifies sample preparation and uses a high throughput STEM detector in a Scanning Electron Microscope (SEM) coupled with commercially available software. In this paper, we demonstrate STEM-VQ with an alphavirus stock preparation to present the method's accuracy and reproducibility, including a comparison of STEM-VQ to viral plaque assay and the ViroCyt Virus Counter.

1. Introduction

Quantitation is an important factor when studying the environmental impact of viruses, or virus impact on a specific host (Ferris et al., 2002; Malenovska, 2013; Rossi et al., 2015). An accurate method for the quantitation of virus particles would be very useful, but a universally accepted method has not been adopted by the scientific community (Ferris et al., 2002; Malenovska, 2013; Rossi et al., 2015; Bettarel et al., 2000). Routinely, multiple different methods of quantitation have been used to substantiate the validity of the other methods. Commonly used methods for virus quantitation includes negative staining Transmission Electron Microscopy (TEM) counting, agar overlay plaque assay, quantitative reverse transcription-polymerase chain reaction (qRT-PCR), immunofluorescence microscopy, Endpoint dilution assay (TCID₅₀) and analytical flow cytometry (Ferris et al., 2002; Malenovska, 2013; Rossi et al., 2015; Kwon et al., 2003; Reid et al., 2003). Direct EM quantitation is a valuable technique because it

provides enumeration of all virus particles, those that are infectious, and those that are non-infectious (Malenovska, 2013; Rossi et al., 2015; Borsheim et al., 1990). However, standardized methods for EM virus quantitation have not been universally implemented, and current techniques can yield inconsistent results with a low limit of detection (Malenovska, 2013; Rossi et al., 2015; Reid et al., 2003). To address the shortcomings of inconsistency and limit of detection, we developed the STEM-VQ method. This is an efficient, reproducible SEM quantitation method which combines mPrep/g capsules to improve and simplify sample preparation with a STEM detector in an SEM for automated image acquisition (Monninger et al., 2016). TEM particle counting was first documented in the 1940s using a spray or centrifugation technique to deposit the sample on the supporting media, followed by negative staining with 2% Uranyl Acetate (Malenovska, 2013; Sharp, 1949; Backus and Williams, 1950; Gelderblom et al., 1991; Miller, 1982). Virus particles within representative fields were imaged with a TEM and manually counted. The final concentration was calculated based on

* Corresponding author.

E-mail address: mei.g.sun.ctr@mail.mil (M.G. Sun).

¹ Current address: General Dynamics Information Technology, 321 Ballenger Center Drive, Frederick, MD, 21702, United States.

² Current address: Army Public Health Center, Toxicology Directorate, 5158 Blackhawk Road, Aberdeen Proving Ground, MD 21010-5403, United States.

the area imaged and the volume of sample applied (Sharp, 1949; Backus and Williams, 1950; Miller, 1982; Kellenberger and Arber, 1957; Mathews and Buthala, 1970; Strohmaier, 1967; Zheng et al., 1996). Since that time, scientists have continued to adapt application techniques to improve sample distribution and different purification steps to decrease sedimentation that interfered with imaging and counting (Mathews and Buthala, 1970; Strohmaier, 1967). In 1950, scientists began using a known concentration of latex beads as a reference within their sample. This allowed calculations based on the bead concentration instead of the area imaged (Backus and Williams, 1950; Gelderblom et al., 1991; Miller, 1982; Kellenberger and Arber, 1957). Inclusion of these reference beads led to development of the droplet method for sample application (Miller, 1982). Several variations have been developed, but the most common method involves placing a drop of sample onto a horizontally oriented grid (Miller, 1982; Zheng et al., 1996). While other methods of counting have been used, typically, the two main approaches for counting TEM images involve either counting a set number of grid squares or a set number of beads. Thresholds for each of these methods have been as few as 3 grid squares, or 200 beads, respectively (Malenovska, 2013; Zheng et al., 1996). There have been numerous approaches to calculating the final concentration of virus (Malenovska, 2013; Rossi et al., 2015; Kwon et al., 2003; Reid et al., 2003; Kellenberger and Arber, 1957; Mathews and Buthala, 1970; Strohmaier, 1967; Zheng et al., 1996). With the development of image analysis software and more automated microscopes in recent years, automated image acquisition, analysis, and enumeration has emerged (Ferris et al., 2002). SEM has been used for many years in the quantitation of particles for material sciences samples and STEM imaging has been used for particle counting in cell monolayers, but STEM imaging has not gained widespread use for particle counting material in biology or virology fields (Ferris et al., 2002; Bogner et al., 2007; Carpenter et al., 2009; Peckys and de Jonge, 2011; Datye et al., 2006).

We have developed a consistent, reproducible virus quantitation method called STEM-VQ which simplifies sample preparation and utilizes large throughput STEM detector in the SEM for imaging, and commercially available image analysis software. Briefly, our method continues to use a known concentration of gold beads as a reference, but it involves a different application method with three major steps (Fig. 1A): First, an equal volume of gold beads is mixed with an unknown concentration of virus particles and the mixture is applied to the EM grid using mPrep/g capsules (Monninger et al., 2016; Miller, 1982; Goodman and Kostna, 2011a; Goodman et al., 2015) (Supplementary Fig. 1). Use of the mPrep/g capsules reduces direct handling of grids and allows easy application of samples and buffers. Second, the grids are imaged with a STEM detector in the SEM using the automated ATLAS software. Compared to traditional TEM imaging, STEM detector imaging in the SEM eliminates the need for negative staining and allows easy imaging of a much larger portion of the grid. Third, ImageJ image analysis software is used to enumerate virus and gold particles. These counts are used to determine the virus to gold ratio and calculate the original virus concentration (Fig. 1C). In this study, we present a comparison of the STEM-VQ method to agarose-based viral plaque assay and the ViroCyt Virus Counter 2100 (VC) (ViroCyt, Boulder, CO, USA) (Rossi et al., 2015; Baer and Kehn-Hall, 2014).

2. Material and methods

2.1. Virus suspension preparation

Venezuelan Equine Encephalitis virus (VEEV), INH-9813 strain and Eastern Equine Encephalitis virus (EEEV), V105-00210 strain were received from Dr. Robert Tesh at the University of Texas Medical Branch repository. VEEV INH-9813 was isolated from the serum of an infected individual who presented with clinical symptoms in Columbia, South America in 1995 (Weaver et al., 1996). The virus was isolated following

a single passage in Vero cells. EEEV V105-00210 was isolated from a human case in Massachusetts in 2005, with no passage in animals and a single passage in cell culture (Centers for Disease C. & Prevention, 2006). Western Equine Encephalitis virus (WEEV) McMillan strain was received from the Centers for Disease Control and Prevention, Fort Collins, CO. This virus was originally isolated from a human case in Ontario, Canada in 1941 (Nagata et al., 2006). This virus had a passage history in both animals and cell culture. Biosafety Level (BSL-3) laboratory prepared master virus stocks (MVS), working virus stocks (WVS), and sucrose purified virus stocks (SpVS) virus stocks were prepared using ATCC Vero 76 cells. For MVS and WVS, Vero cells were infected at a multiplicity of infection (MOI) of 1 in Eagles Minimal Essential Medium (EMEM, Cellgro) containing 2% fetal bovine serum (FBS, HyClone), 1% non-essential amino acids (NEAA, Gibco), 1% Penicillin-Streptomycin (Pen-Strep, 10,000 U/ml and 10 mg/ml stock, respectively, Sigma-Aldrich), 1% HEPES buffer (1 M stock, Sigma-Aldrich), and 1% L-glutamine (200 mM stock, HyClone). At 24–32 h post-infection (PI), culture supernatants were harvested and clarified by centrifugation at 10,000 x g for 30 min (Sorvall GSA rotor). Virus stocks were aliquoted and stored at -70°C for future use. The SpVS, supernatant was collected from Vero cells that were infected at a MOI = 1 in EMEM containing 5% FBS, 0.5% Pen-Strep (stock solution above), 1% HEPES (stock solution above), 1% L-Glutamine (stock solution above), and 0.1% Gentamicin (50 mg/ml stock, Sigma-Aldrich) and clarified by centrifugation. Virus was precipitated with 2.3% NaCl and 7% Polyethylene glycol (MW8000, Sigma-Aldrich), with stirring, overnight at 4°C . Virus was pelleted by centrifugation at 10,000 x g for 30 min (Sorvall GSA rotor). Virus pellets were resuspended in $1 \times$ TNE Buffer (10 mM Tris, 0.2 M NaCl, 1 mM EDTA, pH 7.4) and layered onto 20–60% continuous sucrose density gradients. This was spun at $100,000 \times g$, 4°C , for 4 h (SW-28Ti rotor, Beckman). The virus band was collected, aliquoted and stored at -70°C for future use.

For all stocks, deep sequence analysis determined that the sequence of these isolates were consistent with the reported strain of VEEV, EEEV, and WEEV. Additionally, this sequencing analysis demonstrated that the virus stocks did not contain contaminating agents.

2.2. STEM-VQ sample preparation with mPrep/g capsules

Viral stocks were serially diluted at 1:10 in phosphate buffered saline (PBS) with dilution volumes of at least 5 ml to achieve the final dilution for application to EM grids. Two formvar-carbon coated 200 mesh copper EM grids (SPI, Cat#3420C-MB) were inserted into a capsule based-microscopy processing system called mPrep/g (Monninger et al., 2016) (Fig. 1A left, Microscopy Innovation, LLC, WI, Cat#G1600 and F1602). Gold beads (40 nm, Ted Pella Cat#15707-5, 1.461×10^{10} particles/ml concentration certified by Particle Technology Labs) were sonicated for 10 min and transported into biocontainment with grid-loaded mPrep/g capsules along with filters, fixatives, and 1% osmium tetroxide. Step 1, in the biocontainment suite, equal volumes of virus (unknown concentration) and gold beads (known concentration) were well mixed (Fig. 1B) and 40 μl of the resulting suspension aspirated into the mPrep/g capsule while attached to a pipette (Fig. 1A left). Step 2, the pipette with mPrep/g attached was laid on its side for 10 min with grids oriented horizontally for even sample distribution onto grid formvar. Step 3, the pipette was picked up and the plunger pressed to dispense the virus bead mixture into a waste container. An aliquot (40 μl) of fixative (2% glutaraldehyde in water) was then aspirated into capsule, incubated with grids oriented horizontally for 20 min, and then dispensed into a waste container. Three rinse cycles were performed by aspirating and immediately dispensing 40 μl of deionized (dI) water. An extra ten rinse cycles were needed with samples that were dense such as the SpVS conditions. Step 4, the mPrep/g capsule was removed from the pipette and placed, with the lid open, into a 50 ml centrifuge tube containing filter paper soaked in 1% Osmium Tetroxide (OsO_4) suspended in water. The tube was sealed for 1 h



Fig 1. STEM-VQ Method overview. (A) The three major phases that are needed for determining particle concentration are illustrated: (left) sample preparation using mPrep/g system, (middle) STEM imaging in the SEM, (right) Particle counting using imageJ. (B) A mixture of a known concentration of virus stock, followed by application of the mixture onto an EM grid for STEM imaging in the SEM is illustrated. (C) Formula used to calculate the number of unknown viral particles based on the known concentration of gold beads and the virus-gold ratio.

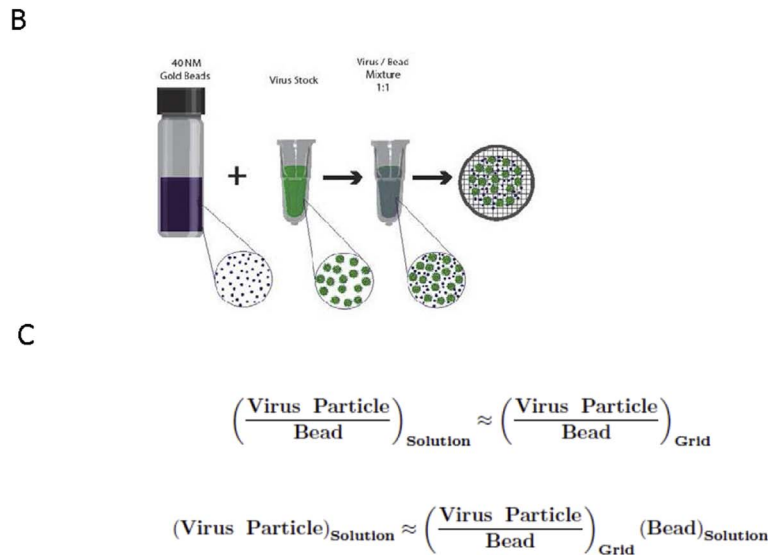
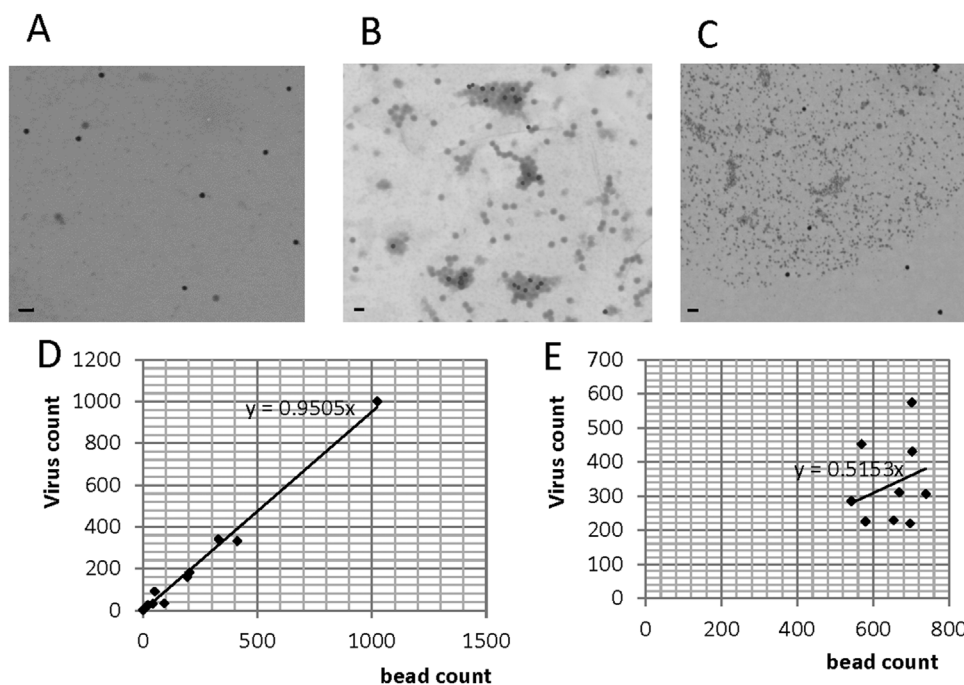


Fig. 2. Good quality sample preparation produces data points that have a strong linear correlation: (A) An example of evenly distributed virus and beads. (B) This sample is too highly concentrated, which leads to clumping and inability to determine an accurate count. (C) This sample contains large amount of crystal sediments and debris in the background; this background material is difficult to differentiate from viral particles when utilizing image analysis software. (D) A strongly correlated data set results from well prepared samples as in A, each data point, 10 total, represents the quantity of virus and beads in a 35 × 35 μm area on a single EM grid. (E) A poorly correlated data set indicates a poorly prepared sample as depicted in panels B and C, each data point, 10 total, represents the quantity of virus and beads in a 35 × 35 μm area on a single EM grid. Scale bars are 100 nm.



to ensure complete inactivation of the virus by OsO₄ vapor and transferred to the BSL-2 electron microscopy facility. Step 5, in the BSL-2 EM facility the mPrep/g capsule was removed from the tube and placed onto a pipette. Three rinse cycles were repeated by aspirating 40 μl of di

water followed by dispensing into a waste container. The capsule was removed from the pipette, lid opened, and allowed to air dry. Once dry, the grids were ready to be imaged under STEM detector in the SEM. (Supplementary Fig. 1) Note, Step 4, inactivation with osmium

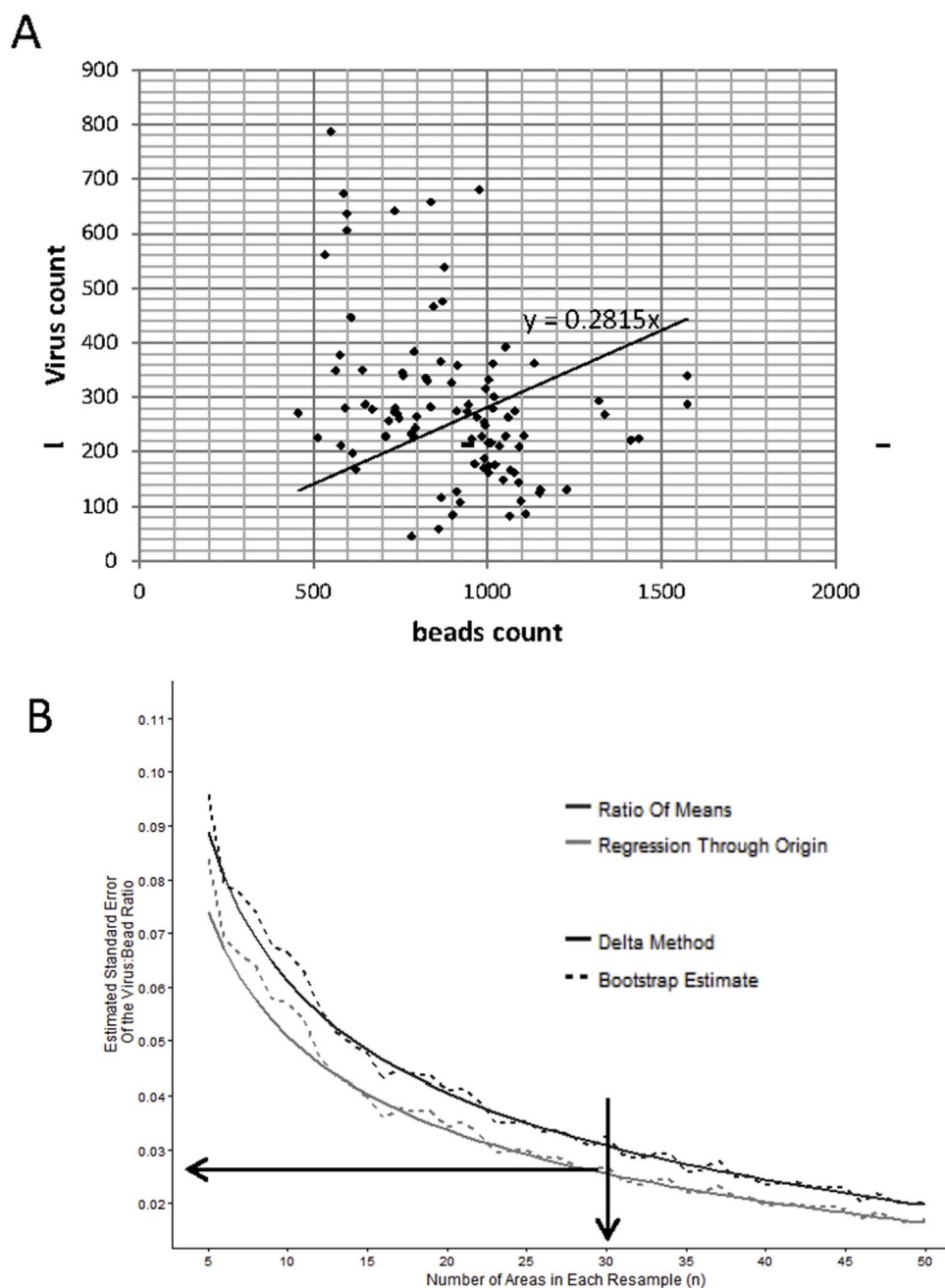


Fig. 3. Computing bootstrapped standard error to statistically determine the number of images required for an accurate STEM-VQ method. (A) Particle count data representing data from 100 imaged areas of a single grid. (B) Bootstrap estimates of the standard error computed by simulating 500 resamples of the 100 areas. Most of the reduction in error is achieved by 30 images.

tetroxide vapor, can be eliminated for samples that do not require BSL-3 or -4 biocontainment.

2.3. STEM imaging

TEM grids were loaded into a Zeiss Sigma Field Emission SEM and imaged with a STEM detector at 30 kV. Images were auto-acquired using Zeiss FIBICS ATLAS software: using $35 \times 35 \mu\text{m}$ frame size, 4 nm/pixel spacing, and 2000 ns dwell time.

2.4. Data analysis by ImageJ

ImageJ software was used to individually count alphaviruses (~70 nm in diameter) and nano-gold particles (~40 nm in diameter) according to their respective particle sizes. Suggested ImageJ macro codes are recorded in supplementary Fig. 3.

2.5. STEM-VQ statistical analysis

2.5.1. Virus to bead ratio

For each grid, the virus to bead' ratio was estimated as the slope of the linear regression of the virus to bead count per sampled grid area, forced through the origin. The sampling variance of the estimated virus to bead ratio obtained from a single grid was taken from the large sample delta-method approximation, as discussed by [van Kempen and van Vliet \(2000\)](#).

$$\text{var}(r_1) \approx \frac{1}{n} \left(\frac{\text{var}(x)}{\mu_y^4} + \frac{\mu_x^2 \text{var}(y)}{\mu_y^4} - \frac{2\mu_x \text{cov}(x, y)}{\mu_y^3} \right)$$

Where x and y are the bead count and the bead weighted virus count and n is the number of sampled areas. Multiple grids were examined per virus sample, an average of the log virus to bead ratio is formed by linear mixed model. This procedure reweights the average to adjust for the correlation observed between certain sets of grids, as well as

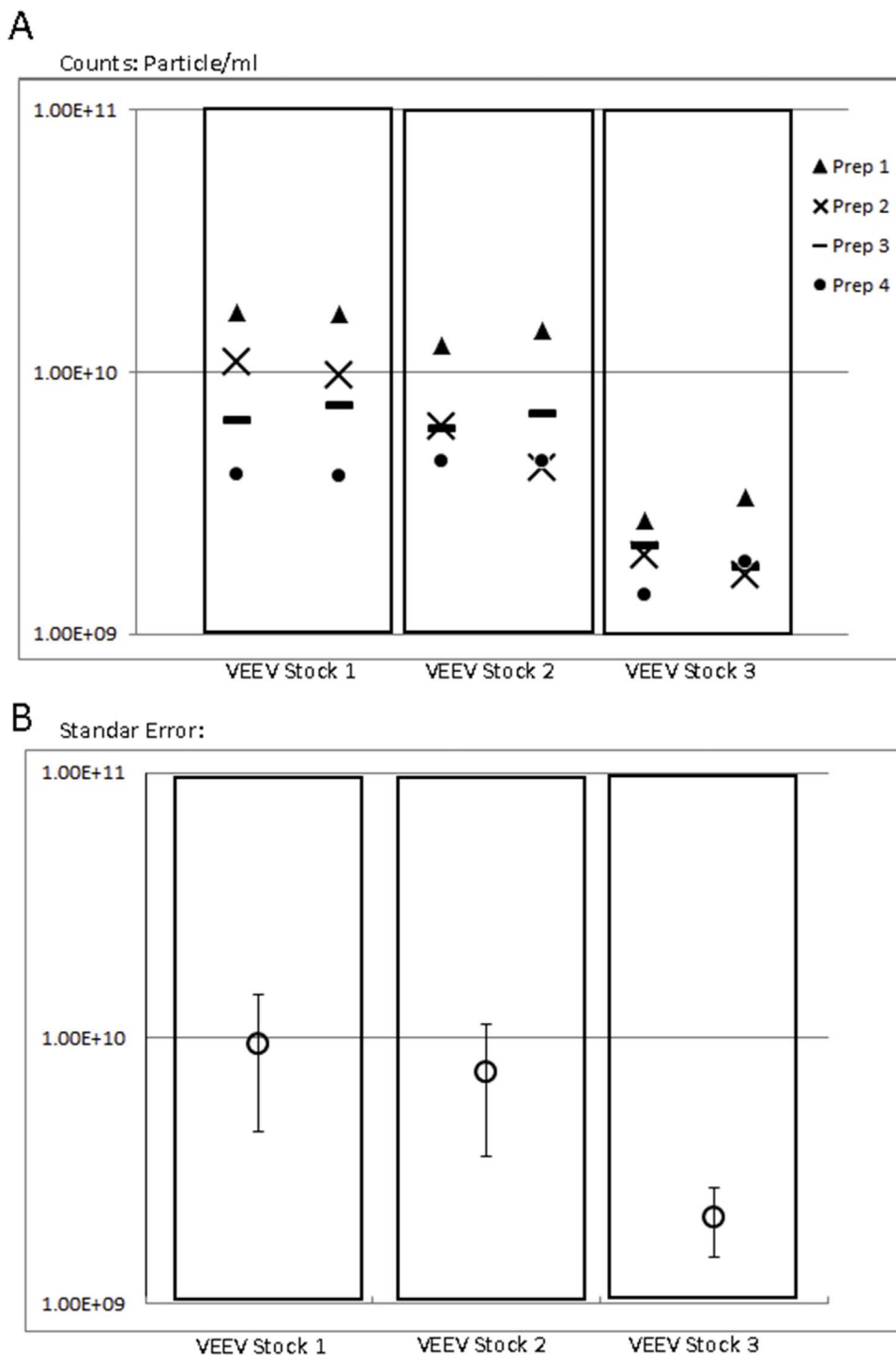


Fig. 4. Individual preparation causes small variations among the same virus stock sample. All counts are calculated from 30 different images per sample. (A) STEM-VQ particle count data of duplicate grids from 3 different individual virus stock samples prepared 4 different times. (B) Standard error from 4 different preparations for the 3 different individual virus stock samples.

sampling variances within grid. Analysis was performed using the PROC MIXED procedure in SAS Version 9.4.

2.5.2. Calculation of the concentration of particles

The following formula is used to calculate the concentration of particles:

$$\text{Unknown Virus Concentration} = \text{Virus to bead ratio} \times \text{Known bead Concentration}$$

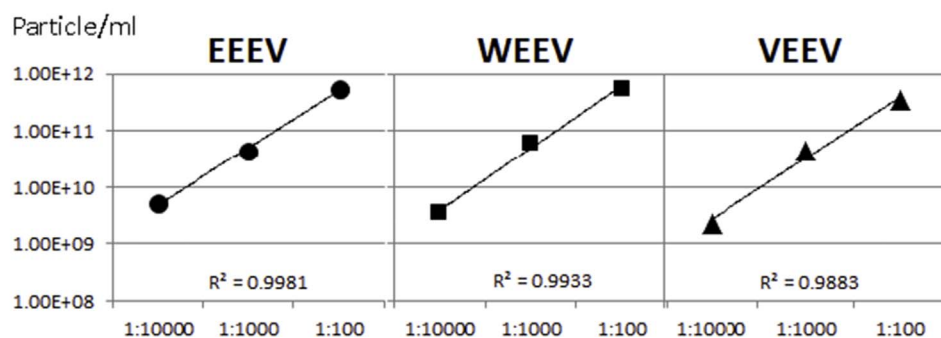
2.6. Agarose overlay plaque assay

Each virus stock was quantitated by standard agarose overlay plaque assay (Baer and Kehn-Hall, 2014). Virus stocks were serially diluted in Hank's Balanced Saline Solution (HBSS). ATCC Vero 76 cells seeded on 6-well plates were grown to 90–100% confluence. Duplicate wells were infected with 100 μ l/well of each serial dilution. Plates were incubated at 37 °C for 1 h, with rocking every 15 min for even distribution and to keep the monolayer from drying. Following the incubation period, wells were overlaid with 0.5% agarose in 2X Eagle's Basal Medium with Earle's Salts (EBME, USAMRIID, Fort Detrick, MD) containing 1% HEPES and 10% FBS, 1% L-glutamine, 1% NEAA, 1% Pen-Strep, and 0.1% gentamycin, and plates incubated at 37 °C with 5%

A

Alphavirus Samples	Dilution	STEM-VQ raw concentration (Particle/ml)
EEEV	1:100	5.34E+11
	1:1000	4.38E+10
	1:10000	5.12E+09
WEEV	1:100	5.47E+11
	1:1000	6.19E+10
	1:10000	3.41E+09
VEEV	1:100	3.37E+11
	1:1000	4.43E+10
	1:10000	2.27E+09

B



CO₂. After twenty four hours the cells were stained with the addition of a second agarose overlay prepared as above with 5% neutral red (Gibco). The plates were incubated at 37 °C with 5% CO₂ for an additional 24 h. Infectivity was quantitated by counting defined plaques (neutral red exclusion areas). Titer was calculated by factoring in the volume of inoculum used per well and the dilution(s) with plaque counts between 10 and 150.

2.7. ViroCyt quantitation

Samples were tested on the VC using the ViroCyt reagent kit and following manufacturer's instructions. The strategy was similar to that described for filoviruses in Rossi et al. (2015). Virus preparations were diluted beginning at 1:10 into ViroCyt sample buffer. Serial ¼ log dilutions were prepared from the 1:10 in order to provide samples with values within the linear range of the VC. Briefly, 300 µl of each dilution was stained using 150 µl of Combo Dye solution, incubated in the dark at room temperature for 30 min, and analyzed in the VC. Each dilution was tested in triplicate with inter-sample washes and a cleanliness control run between each sample to verify the flow path was clean. Results were automatically analyzed by the instrument software and reported as virus particles per ml (VP/ml). The sample quantitation limit (SQL) for unpurified virus stocks were similar to that previously reported for filoviruses (2.0E + 06 VP/ml) while purified virus SQL was lower and equivalent to the lower limit of the linear range of the instrument (5.5E + 05 VP/ml). All VC results greater than this value were considered statistically distinguishable from background and therefore reportable. Final virus particle concentrations were established using all samples whose VP/ml counts were above background and within the linear range of the instrument. Microsoft Excel 2007 (Redmond, WA, USA) was used for linear-regression analysis and determining coefficient of variation between replicates. Instrument performance was validated prior to testing samples by running a manufacturer's control of known concentration.

Fig. 5. STEM-VQ data from different sample dilutions indicate accurate counting result. All counts are calculated from 30 different images per sample. (A) Results from 3 different alphavirus stocks using 3 different dilutions. (B) Comparison of the data from different dilutions.

3. Results

3.1. Sample preparation quality correlated with accuracy

Uniform particle distribution and minimal background on EM grids was critical for achieving accurate results (Fig. 2A and D) (Kwon et al., 2003; Reid et al., 2003; Zheng et al., 1996). Proper sample preparation, including bead agitation, extensive mixing of the gold beads with the virus, and at least 3 washes with reagent grade water was required. Particles aggregation was always a sample preparation problem (Fig. 2B). Sonication of the bead stock prior to mixing with the virus helped to suspend the bead solution and eliminate clumping that formed when the solution was stored for a lengthy period between uses. Thorough mixing of the virus and gold beads by pipetting the mixture up and down several times evenly distributed sample throughout the solution and helped remove any viral aggregation. Nutrient rich media was required for virus growth, but this media resulted in crystallized salt and sugar deposits on the grid which made imaging and counting difficult (Fig. 2C and E). Extra rinsing at least 10 times with water helped eliminate these deposits.

Upon data analysis, we found that correlation strength between the gold bead count and virus count was an indicator of good sample preparation quality; and therefore, result accuracy (Fig. 2D and E). All of the samples used here were well prepared and the standard macro was used. As we have developed this method we have observed that while inferior preparations should be immediately identifiable during imaging, areas within the grid that contain particle clumping or dirty background may go undetected with our automated imaging process. Samples that contained particle aggregation or dirty background are usually identified by the technician when the data set is poorly correlated or contains extreme outliers (Fig. 2E). In this event, the image analysis can be adjusted in a manner appropriate to the severity of the issue. Adjustments to the analysis macro code (Supplementary Fig. 3) such as tailored thresholding or background extraction often solves the issue. If the particle aggregation or dirty background is severe enough a

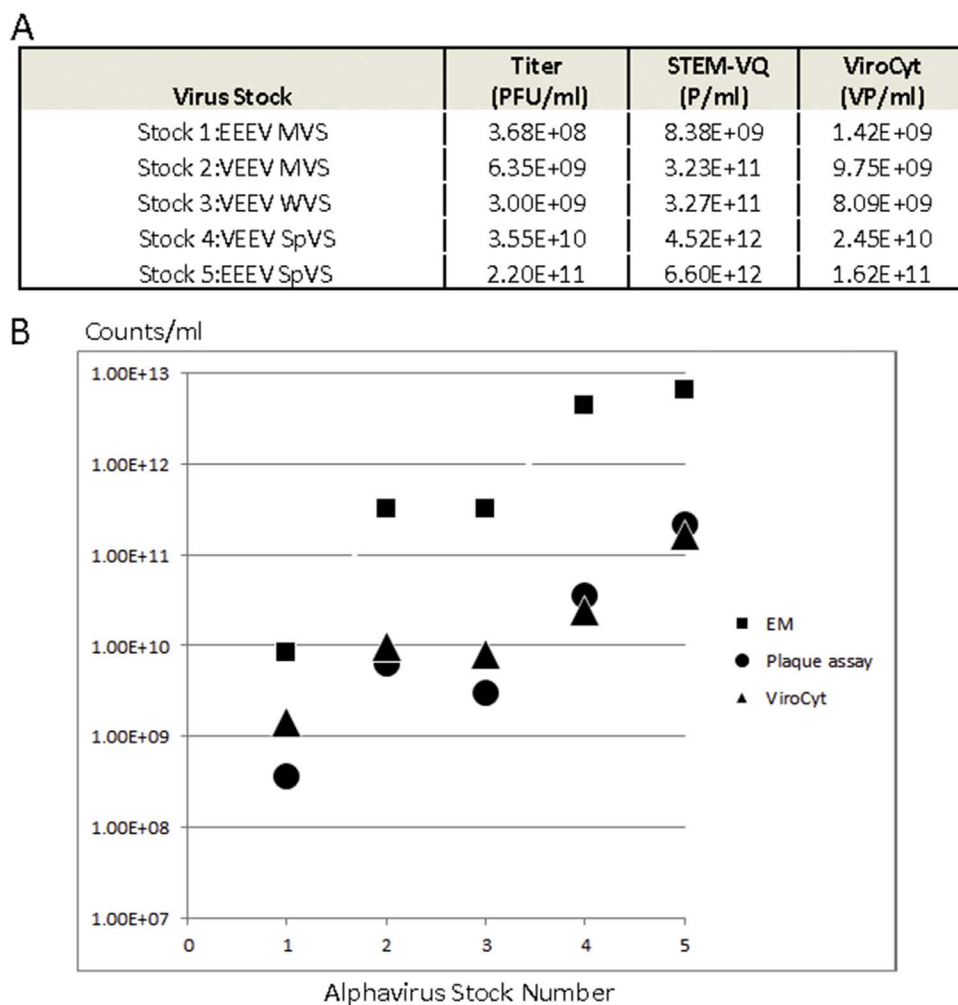


Fig. 6. STEM-VQ method results are consistent with plaque assay and ViroCyt counting results. (A) Quantitation results for 5 different alphavirus stocks using 3 different quantitation methods. All EM counts are calculated from 30 different images per sample. (B) Comparison of the results from different methods in graphical format. EM results are higher than ViroCyt and plaque assay because it counts the presence of all particles, including non-infectious.

new grid preparation for imaging is required.

3.2. Computing bootstrapped standard error to statistically determine the number of images for an accurate STEM-VQ calculation

One-hundred areas were imaged from a single grid to determine the number of imaged areas that would be required for an accurate representation of the entire grid (Fig. 3A). Two possible estimators of the virus to bead ratio were compared: (1) the ratio of mean virus count to mean bead count (ratio of means) and (2) the slope of the linear regression of virus to bead counts, forced through the origin (regression through the origin). The 100 areas were resampled 50 times with replacement to form a boot-strap estimate of the standard error (Fig. 3B) (Wasserman, 2006). As shown in Fig. 3B, the standard error decreased with increasing numbers of sampled areas. Considering a compromise between the costs of increased sampling versus the reduction in error, we determined that 30 imaged areas per grid were needed for accurate quantitation. Most of the gains in reliability were realized by $n = 30$, with further increases in the number of sampled areas yielding only small reductions in variance.

3.3. Individual sample preparations result in variation and limited analytical errors

We found that a major source of error came from the variability between sample preparations. We analyzed 4 different preparations of 3 different individual VEEV stock samples. Each preparation consisted of two duplicate grids (Fig. 4A). The results from the simultaneously

prepared duplicate grids in each preparation were very similar to each other, but there were variations between different preparations. Fig. 4B shows the standard error calculated from the counts in Fig. 4A. The range varied between one standard error above and one standard error below demonstrating that the variability was less than a log, which is commonly considered acceptable for EM particle counts (Malenovska, 2013; Rossi et al., 2015; Darling et al., 1998).

3.4. Detection limit for accurate counting

The detection limit for any EM procedure is typically considered $1E + 07$ particles/ml (P/ml) (Malenovska, 2013; Reid et al., 2003). In order to determine the range for accurate counting for the STEM-VQ method, we examined serial dilutions using alphavirus samples (Fig. 5A). We found that samples containing greater than $1E + 12$ P/ml typically had too much viral aggregation for an accurate quantitation (data not shown). At the lower end, samples below $1E + 07$ P/ml had too few viral particles in the field of view for an accurate count (data not shown). Particle counts within the range of $1E + 09$ to $1E + 12$ P/ml provided accurate detection in 10-fold dilutions for three different sucrose-purified virus stocks (EEEV, WEEV and VEEV) (Fig. 5B). All data in serial dilutions were linear, indicating the accuracy of the data set.

3.5. STEM-VQ method results were comparable to agarose-based plaque assay and ViroCyt virus counter results

There are many ways to quantify virus, all of which use very

different methods to identify particles. Among all methods, plaque assay and the VC are well developed and widely used. Plaque assay is the most common approach to virus quantitation and is typically considered the “gold standard” (Malenovska, 2013; Rossi et al., 2015). It measures infectious virus particles by counting the number of plaques formed when virus is applied to a monolayer of cells, giving a count expressed as plaque forming units per ml (PFU/ml) (Malenovska, 2013; Rossi et al., 2015; Bettarel et al., 2000). The VC is a flow-based counter which quantifies virus particles in solution (Rossi et al., 2015). It requires the sample to be stained for protein and nucleic acid and counts particles containing both stains as intact virus particles, resulting in a count expressed as virus particles per ml VP/ml (Rossi et al., 2015). With STEM-VQ particle images are captured and particles counted electronically, then visually confirmed. Counts are expressed as particles per ml P/ml (Malenovska, 2013).

We compared STEM-VQ, plaque assay and VC results for different alphavirus stocks (Fig. 6). The linear range of the VC was verified to be between $5.5E + 05$ and $1E + 09$ VP/ml. Testing of each virus prep resulted in a linear curve with $R^2 \geq 0.972$, slopes between 0.916 and 1.396 and coefficient of variation (%CV) $\leq 29\%$ using at least 4 concentrations and n between 11 and 18. Since the plaque assay measures infectious particles and the VC counts essentially intact virus particles, we expected VC and plaque assay results to be similar for each virus stocks. Our data agreed with this theory. We also expected the STEM-VQ results to be higher than both plaque assay and the VC since STEM-VQ counts the presence of all particles within a size range and cannot determine if they are infectious. We consistently found STEM-VQ results approximately 1.5 logs higher than the plaque assay and VC results (Fig. 6). We do not propose that all types of viruses or variable conditions would result in a 1.5 log difference in plaque assay and EM counting, but we would always expect the EM count to be higher than plaque assay.

4. Discussion

Virus quantitation using negative stain TEM imaging has been criticized as difficult and time consuming; issues we wanted to improve with the development of this method. In supplementary Fig. 2, we compared and summarized the improvements made to the STEM-VQ method compared to the conventional TEM method. We simplified sample preparation with better distribution by using mPrep/g capsules in the process. The mPrep/g is a small capsule that functions as a pipette tip capable of holding two EM grids (Goodman and Kostrna, 2011b) (Fig. 1A left). Once the grids have been inserted into the capsule, the person preparing the sample simply attaches the mPrep/g capsule to a pipette and no further grid manipulation is needed. Using mPrep/g resulted in much less damage to the grid during sample preparation, providing more data available to collect for more accurate results. It also made sample preparation in biocontainment labs (BSL3 and BSL4) much safer and easier. Each capsule holds 2 grids; therefore, duplicate grids can be made with no further effort. The capsules can also easily be loaded onto a multi-channel pipette, or stacked, so many samples or several replicates of the same sample can easily be prepared (Goodman and Kostrna, 2011b). Additionally, uniform particle distribution on the grid is critical for achieving accurate data (Kwon et al., 2003; Reid et al., 2003; Zheng et al., 1996). We found samples prepared using the capsule consistently showed more uniform distribution than samples prepared using the traditional droplet method (Monninger et al., 2016).

Our new automated imaging and analysis procedure saved valuable technician time and allowed for the collection of larger data set in a shorter period of time. ATLAS automated imaging software enabled the user to select multiple areas to image, optimize the image acquisition settings for quality imaging such as focus, brightness, and contrast, and then the software automatically acquired images from large areas of the sample while unattended. We were able to acquire images of thirty

$35 \times 35 \mu\text{m}$ square areas from a 200 mesh grid in less than 3 h, and a technician needed to be present for only 45 min of those 3 h. This was significantly less time when compared to traditional methods in which a technician must continually sit at the microscope manipulating the controls and taking individual images. This new method not only saved time but largely decreased the amount of hands-on time required by a technician. Similarly, ImageJ analysis decreased the time needed to count the particles. Manually counting a well populated grid square requires hours of counting, whereas, using ImageJ software the same images were completed in less than 5 min. When counting or imaging is manually performed, accidental overlap or skipping an area frequently occurs. Utilization of software for analysis and automated image acquisition eliminated this error.

Virus quantitation is an important step when characterizing challenge material for use in animal models of infectious disease. There are many methods for virus quantitation including plaque assay, TCID₅₀, the VC, and EM (Ferris et al., 2002; Malenovska, 2013; Rossi et al., 2015; Kwon et al., 2003; Reid et al., 2003). The desired information and practicality of each method should be considered when determining which method to use. The plaque assay can be time consuming, typically requiring many days to complete, and must be performed at the level of containment appropriate for the virus being handled (Malenovska, 2013; Rossi et al., 2015). Choosing a cell line, media, and other variables are essential to a successful plaque assay (Rossi et al., 2015). Plaque assay has the lowest limit of detection (Dulbecco, 1952). It can only detect infectious particles, which a majority consider more applicable for dosing quantitation because infectious particles are responsible for disease; however, there is evidence that noninfectious particles can also effect the host immune response (Alfson et al., 2015). Therefore, it is important to evaluate noninfectious as well as infectious particles present in virus challenge stock preparations.

For alphaviruses, the VC results were comparable to plaque assay results, but VC has a higher limit of detection with an optimal range of $5.5E + 5$ – $1.0E + 9$ VP/ml (Rossi et al., 2015). It must also be operated in the level of containment required for the sample, but it was quick, taking less than an hour to stain and count a sample. It was also the most affordable option, costing about \$5.00 per run. However, the VC may provide poor results in samples with high levels of protein in the media (Rossi et al., 2015).

A major limitation of EM counting methods despite improvements seen with the STEM-VQ method is the relatively high detection limit, a concentration of $1E + 07$ P/ml remains necessary for accurate results (Malenovska, 2013; Reid et al., 2003). Media containing high levels of salt, protein, or sucrose may lead to poor imaging if not properly rinsed, and poor fixation can lead to loss of sample from the grid or unidentifiable particles (Malenovska, 2013; Kwon et al., 2003). After BSL-3/4 sample application to the grid, which takes about an hour, exposure to osmium tetroxide vapor quickly deactivates any virus and allows the rest of the work to be performed outside biocontainment (Monninger et al., 2016).

Despite its challenges, EM quantitation is valuable due to its ability to count total virus particles and provide gross morphology data. It should be noted that although this method allowed for gross morphological evaluation; more detailed observations such as protein coat on virus particles requires additional EM procedures such as negative staining with TEM imaging. These EM methods can also be applied to other noninfectious nano-particles such as virus-like-particles (VLPs), whereas plaque assays and VC are unable to quantify VLPs. EM may also be able to provide insight into VLPs development or changes due to manipulations through morphologic evaluation (Pease et al., 2009; Roldao et al., 2010). STEM-VQ and VC particle counts can be used in conjunction with other quantitation methods, typically plaque assay, to create ratios that provide insight into both infectivity of a virus stock and the quality of the virus preparation. These ratios (P:PFU and VP:PFU) are important when examining alterations in the quality of virus stocks which can arise from mutation, poor handling techniques,

or sequential passaging (Carpenter et al., 2009; Thompson and Yin, 2010; McCurdy et al., 2011).

The STEM-VQ method simplifies sample preparation, imaging, and data analysis for particle analysis using electron microscopy. These changes have increased the accuracy and reproducibility of the assay.

Additional information

Competing financial interest statement: The authors declare no competing financial interests.

Acknowledgements

We would like to acknowledge Dr. Camenzind Robinson (Janelia Research Campus, Howard Hughes Medical Research Institute) for his input and initial STEM set up for this project. We would like to thank SPC Joshua Patterson for helping proof read this manuscript. This work was funded in part by USAMRIID and the Defense Threat Reduction Agency-Joint Science and Technology Office (Program CB3691).

Opinions, interpretations, conclusions, and recommendations are those of the authors and are not necessarily endorsed by the U.S. Army.

Appendix A. Supplementary data

Supplementary data associated with this article can be found, in the online version, at <http://dx.doi.org/10.1016/j.jviromet.2017.06.014>.

References

- Alfson, K.J., et al., 2015. Particle-to-PFU ratio of Ebola virus influences disease course and survival in cynomolgus macaques. *J. Virol.* 89, 6773–6781.
- Backus, R.C., Williams, R.C., 1950. The use of spraying methods and of volatile suspending media in the preparation of specimens for electron microscopy. *J. Appl. Phys.* 21, 11–15.
- Baer, A., Kehn-Hall, K., 2014. Viral concentration determination through plaque assays: using traditional and novel overlay systems. *J. Vis. Exp.* e52065.
- Bettarel, Y., Sime-Ngando, T., Amblard, C., Laveran, H., 2000. A comparison of methods for counting viruses in aquatic systems. *Appl. Environ. Microbiol.* 66, 2283–2289.
- Bogner, A., Jouneau, P.H., Thollet, G., Basset, D., Gauthier, C., 2007. A history of scanning electron microscopy developments: towards wet-STEM imaging. *Micron* 38, 390–401.
- Borsheim, K.Y., Bratbak, G., Heldal, M., 1990. Enumeration and biomass estimation of planktonic bacteria and viruses by transmission electron microscopy. *Appl. Environ. Microbiol.* 56, 352–356.
- Carpenter, J.E., Henderson, E.P., Grose, C., 2009. Enumeration of an extremely high particle-to-PFU ratio for Varicella-zoster virus. *J. Virol.* 83, 6917–6921.
- Darling, A.J., Boose, J.A., Spaltro, J., 1998. Virus assay methods: accuracy and validation. *Biologicals* 26, 105–110.
- Datye, A.K., Xu, Q., Kharas, K.C., McCarty, J.M., 2006. Particle size distributions in heterogeneous catalysts: what do they tell us about the sintering mechanism? *Catal. Today* 111, 59–67.
- Dulbecco, R., 1952. Production of plaques in monolayer tissue cultures by single particles of an animal virus. *Proc. Natl. Acad. Sci. U. S. A.* 38, 747–752.
- Ferris, M.M., Stoffel, C.L., Maurer, T.T., Rowlen, K.L., 2002. Quantitative intercomparison of transmission electron microscopy, flow cytometry, and epifluorescence microscopy for nanometric particle analysis. *Anal. Biochem.* 304, 249–256.
- Gelderbloom, H.R., Renz, H., Özel, M., 1991. Negative staining in diagnostic virology. *Micron Microsc. Acta* 22, 435–447.
- Goodman, S.L., Kostrna, M.S., 2011a. Reducing reagent consumption and improving efficiency of specimen fixation and embedding, grid staining and archiving using mPrep capsule processing. *Microsc. Microanal.* 17, 174–175.
- Goodman, S., Kostrna, M., 2011b. Reducing reagent consumption and improving efficiency of specimen fixation and embedding, grid staining and archiving using mPrep (TM) capsule processing. *Microsc. Microanal.* 17 (1174).
- Goodman, S.L., Wendt, K.D., Kostrna, M.S., Radi, C., 2015. Capsule-based processing and handling of electron microscopy specimens and grids. *Microscopy Today* 23, 30–37.
- Kellenberger, E., Arber, W., 1957. Electron microscopical studies of phage multiplication. I. A method for quantitative analysis of particle suspensions. *Virology* 3, 245–255.
- Kwon, Y.J., Hung, G., Anderson, W.F., Peng, C.A., Yu, H., 2003. Determination of infectious retrovirus concentration from colony-forming assay with quantitative analysis. *J. Virol.* 77, 5712–5720.
- Malenovska, H., 2013. Virus quantitation by transmission electron microscopy, TCID₅₀ (0), and the role of timing virus harvesting: a case study of three animal viruses. *J. Virol. Methods* 191, 136–140.
- Mathews, J., Buthala, D.A., 1970. Centrifugal sedimentation of virus particles for electron microscopic counting. *J. Virol.* 5, 598–603.
- McCurdy, K., et al., 2011. Differential accumulation of genetic and phenotypic changes in Venezuelan equine encephalitis virus and Japanese encephalitis virus following passage in vitro and in vivo. *Virology* 415, 20–29.
- Miller, M., 1982. Virus particle counting by electron microscopy. *Electron Microscopy Biol.* 2, 305–339.
- Monninger, M.K., et al., 2016. Preparation of viral samples within biocontainment for ultrastructural analysis: utilization of an innovative processing capsule for negative staining. *J. Virol. Methods* 238, 70–76.
- Nagata, L.P., et al., 2006. Infectivity variation and genetic diversity among strains of Western equine encephalitis virus. *J. Gen. Virol.* 87, 2353–2361.
- Pease 3rd, L.F., et al., 2009. Quantitative characterization of virus-like particles by asymmetrical flow field flow fractionation, electrospray differential mobility analysis, and transmission electron microscopy. *Biotechnol. Bioeng.* 102, 845–855.
- Peckys, D.B., de Jonge, N., 2011. Visualizing gold nanoparticle uptake in live cells with liquid scanning transmission electron microscopy. *Nano Lett.* 11, 1733–1738.
- Centers for Disease C. & Prevention, 2006. Eastern equine encephalitis—New Hampshire and Massachusetts, August–September 2005. *MMWR. Morb. Mortal. Wkly. Rep.* 55, 697–700.
- Reid, G.G., et al., 2003. Comparison of electron microscopic techniques for enumeration of endogenous retrovirus in mouse and Chinese hamster cell lines used for production of biologics. *J. Virol. Methods* 108, 91–96.
- Roldao, A., Mellado, M.C., Castilho, L.R., Carrondo, M.J., Alves, P.M., 2010. Virus-like particles in vaccine development. *Expert Rev. Vaccines* 9, 1149–1176.
- Rossi, C.A., et al., 2015. Evaluation of ViroCyt(R) Virus Counter for rapid filovirus quantitation. *Viruses* 7, 857–872.
- Sharp, D.G., 1949. Enumeration of virus particles by electron micrography. *Proc. Soc. Exp. Biol. Med.* 70, 54–59.
- Strohmaier, K., 1967. A new procedure for quantitative measurements of virus particles in crude preparations. *J. Virol.* 1, 1074–1081.
- Thompson, K.A., Yin, J., 2010. Population dynamics of an RNA virus and its defective interfering particles in passage cultures. *Virol. J.* 7, 257.
- Wasserman, L., 2006. *All of Nonparametric Statistics*. Springer-Verlag, New York, NY, pp. 27–39.
- Weaver, S.C., et al., 1996. Re-emergence of epidemic venezuelan equine encephalomyelitis in South America. VEE study group. *Lancet* 348, 436–440.
- Zheng, Y.Z., Webb, R., Greenfield, P.F., Reid, S., 1996. Improved method for counting virus and virus like particles. *J. Virol. Methods* 62, 153–159.
- van Kempen, G.M., van Vliet, L.J., 2000. Mean and variance of ratio estimators used in fluorescence ratio imaging. *Cytometry* 39, 300–305.